This is an open access article published under an ACS AuthorChoice License, which permits copying and redistribution of the article or any adaptations for non-commercial purposes.

ACS OMEGA

Article

Cite This: ACS Omega 2018, 3, 13711−13719

http://pubs.acs.org/journal/acsodf

One-Pot Magnetic Iron Oxide−Carbon Nanodot Composite-Catalyzed Cyclooxidative Aqueous Tandem Synthesis of Quinazolinones in the Presence of *tert*-Butyl Hydroperoxide

Biju Majumdar, Daisy Sarma, Siddarth Jain, and Tridib K. Sarma*

Discipline of Chemistry, Indian Institute of Technology Indore, Simrol, Khandwa Road, Indore 453552, Madhya Pradesh, India

Supporting Information

ABSTRACT: The development of synthetic protocols for biologically important molecules using biocompatible catalysts in aqueous medium holds the key in green and sustainable chemistry. Herein, a magnetically recoverable iron oxide−carbon dot nanocomposite has been demonstrated as an effective catalyst for cyclooxidative tandem synthesis of quinazolinones in aqueous medium using alcohols as starting materials. Fluorescent carbon dots, the newest entrant in the nanocarbon family, were used as the stabilizing agent for the iron oxide nanoparticles, and a continuous layer of carbon dots decorates the iron oxide nanoparticle surface as observed by transmission electron microscopy. The fluorescence studies demonstrated the effective electron transfer from carbon dots to the iron oxide nanoparticles resulting in complete quenching of emission owing to carbon dots, once it binds with iron oxide nanoparticles. The nanocatalyst showed high activity with significant reusability for the syntheses of quinazolinones in the presence of *tert*-butyl hydroperoxide (TBHP) in an aqueous medium. Controlled experiments revealed the synergistic effect of carbon dots in enhancing the catalytic activity of iron oxide, as they might influence the decomposition of TBHP into radicals owing to their peroxidase activity. These radicals stabilized over the nanoparticle surface are known to have increased lifetime compared to solution-based radicals. These surface-stabilized radicals then could catalyze the tandem reaction resulting in the formation of the quinazolinone derivatives in high yields.

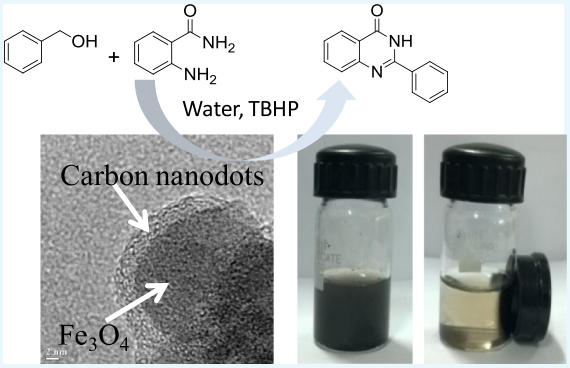

INTRODUCTION

In recent years, there has been a tremendous emphasis toward developing greener methodologies in industrial production of fine and commodity chemicals.[1−3] The focal point to attain a clean and sustainable method has been toward the use of safer solvents, most preferably water, and the use of nontoxic and recyclable catalyst. Following these principles, there is a considerable interest toward the development of transition metal oxide nanocatalysts in cascade organic synthesis. Amidation of C(sp^3)−H bonds leading to N-heterocycles, similar to quinazolinones, represent an important organic transformation. The traditional C−H amidation reactions involve several drawbacks, such as functionalization of starting materials, use of stoichiometric amounts of metal catalysts, and hazardous solvents. On the other hand, direct C−H amidation has received substantial interests because of reduced number of synthetic steps and does not require excessive catalyst amount.[4−8] Quinazolinones have an important motif in several biologically relevant pharmacophores and exhibit a broad spectrum of activities such as anticancer, antiviral, anti-inflammatory, and antimicrobial activity (Scheme 1a).[9−13] The classical method of quinazolinone synthesis involves condensation of aldehydes and 2-aminobenzamides to give aminal intermediates, which then undergo oxidation to yield the final quinazolinone product.[12,13] However, the use of chemically unstable aldehydes as a starting material and hazardous oxidants, such as $KMnO_4$, $CuCl_2$, and 2,3-dichloro-5,6-dicyano-1,4-benzoquinone, are significant limitations in this method. Another strategy is to use more benign and readily available alcohols as starting materials.[14] The reaction takes place through a two-step oxidation pathway, where alcohols are first oxidized to aldehydes, followed by coupling with 2-aminobenzamides forming an aminal derivative and their oxidation to the final quinazolinone. The catalyst needs to demonstrate high activity and selectivity as the reaction involves dehydrogenation of both C−H and N−H bond in one pot. Various homogeneous and heterogeneous systems including ZnI_2,[15] homogeneous Ru and Pd catalysts, iron salts,[16−19] heterogeneous Pt nanoclusters,[20] $[Cp^*IrCl_2]_2$,[21] and organocatalytic domino strategies[22,23] have been developed for quinazolinones. Although these approaches resulted in an excellent formation of the product, the reaction involved the use of precious metal catalysts with high loading, toxic solvents, hazardous byproducts, or complexity in work-up. Therefore,

Received: July 27, 2018
Accepted: October 3, 2018
Published: October 19, 2018

© 2018 American Chemical Society

DOI: 10.1021/acsomega.8b01794
ACS Omega 2018, 3, 13711−13719

Scheme 1. (a) Selected Examples of Biologically Active Quinazolinones and (b) One-Pot Synthesis of Quinazolinones with Alcohols and 2-Aminobenzamides as the Starting Materials

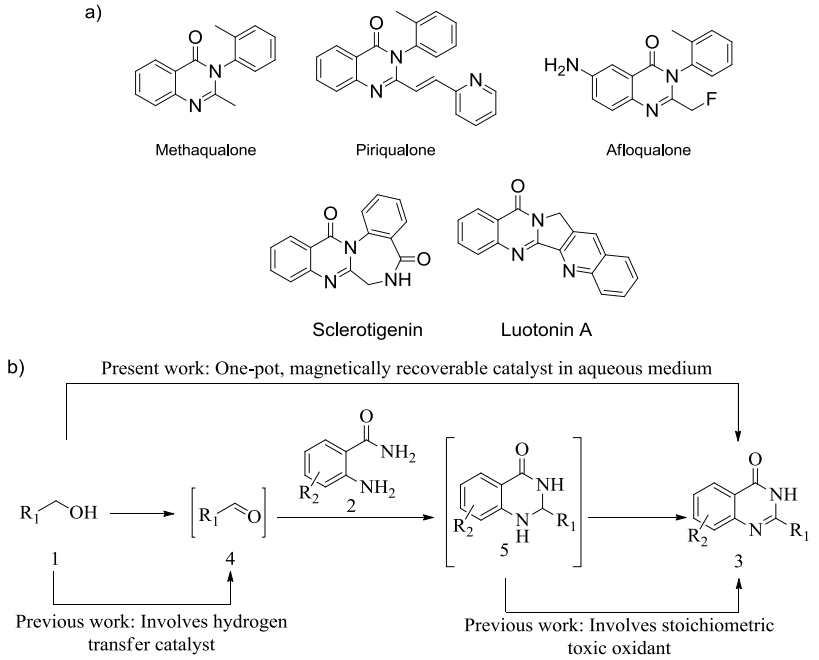

there has been a great scope for the development of greener synthetic procedures using easily separable heterogeneous catalysts using water as the reaction medium. Water is the most acceptable solvent for sustainable synthetic chemistry because of their natural abundance, no toxicity as well as reduced work-up simplicity and purification process.[24−29] Keeping all of these points in mind, development of an easily recoverable, stable, low cost, and heterogeneous catalytic system (Scheme 1b) from earth-abundant metals for the formation of important compounds such as quinazolinones in water is highly desirable.

Low-cost and environmentally friendly Fe_3O_4 nanocatalysts have demonstrated high efficiency toward several organic reactions.[30−33] The easy removal and reusability of these magnetic nanoparticles from the reaction mixture by magnetic separation is an important criterion for ecological and economical demands. On the other hand, carbon nanodots (CNDs), the fluorescent tiny form of nanocarbons, have attracted a wide variety of applications in the technologically relevant areas such as optoelectronic devices, solar cells, sensing, bioimaging, and so forth.[34−38] The high dispersibility in water, biocompatibility, and photostability make this material an attractive alternative to the semiconductor quantum dots for these applications. Further, CNDs demonstrate excellent peroxidise activities that have been harnessed for biological sensing.[39,40] Earlier, we reported the activity of CNDs for the reduction of metal salts to form metal nanoparticles that were used for catalysis and sensing applications.[41,42] CNDs also demonstrate excellent carbocatalytic activity for various organic transformations owing to their inherent acidic and oxidative properties.[43,44] The presence of carboxylic functionality on the CND surface makes them an effective stabilizer for oxide nanoparticles, and cooperative interactions might influence the activity of the metal oxides as catalysts. Herein, we demonstrate that CND-stabilized Fe_3O_4 nanoparticles could be used as an efficient catalytic system for one-pot tandem reaction leading to quinazolinones from alcohols as starting materials. Most importantly, the formation of quinazolinones could be accomplished in an aqueous medium using *tert*-butyl hydroperoxide (TBHP) as an external oxidant. Recently, nanocrystalline MnO_2 has shown good activity as a heterogeneous catalyst for the synthesis of quinazolinone in the presence of TBHP;[45] however, the reactions were performed using toxic chlorobenzene as a solvent. CNDs not only function as effective surface-stabilizing agents for the Fe_3O_4 nanoparticles but also contribute to the enhancement of catalytic activity of the composite through their intrinsic peroxidise activity. Thus, the present method represents substantial improvements over the earlier reported methods from green and sustainable chemistry point of view.

RESULTS AND DISCUSSION

Synthesis and Characterization of Catalysts. Toward the development of the magnetic nanocatalytic system, we first synthesized −COOH surface-functionalized CNDs by microwave treatment of polyethylene glycol-200 (PEG-200) in a focused microwave CEM discover reactor at 150 W and 150 °C for 30 min. The synthesized brown dispersion demonstrated excitation-dependent emission behavior with the maximum emission, observed at 490 nm at an excitation wavelength of 375 nm (Figure 1a).[46] Transmission electron microscopy (TEM) also validated the generation of well-dispersed spherical NPs (Figure 1b) with the average particle diameter of 3.4 ± 0.7 nm. It is well-known that caramelization of PEG leads to the formation of carboxyl group-functionalized surfaces on the carbonaceous structures,[47] which can be used as an effective stabilizer for the oxide materials. Therefore, CNDs were directly used as a passivating agent for iron oxide nanoparticles. The synthesis of Fe_3O_4 nanoparticles was performed using the well-known coprecipitation method using a mixture of Fe^{3+} and Fe^{2+} salts (2:1) in an aqueous medium using CNDs as stabilizing agents. From the TEM studies, the formation of spherical Fe_3O_4 NPs was clearly evident having an average diameter of 10 ± 0.8 nm (Figure 1c). A wrapping high-contrast Fe_3O_4 core was wrapped by a

DOI: 10.1021/acsomega.8b01794
ACS Omega 2018, 3, 13711−13719

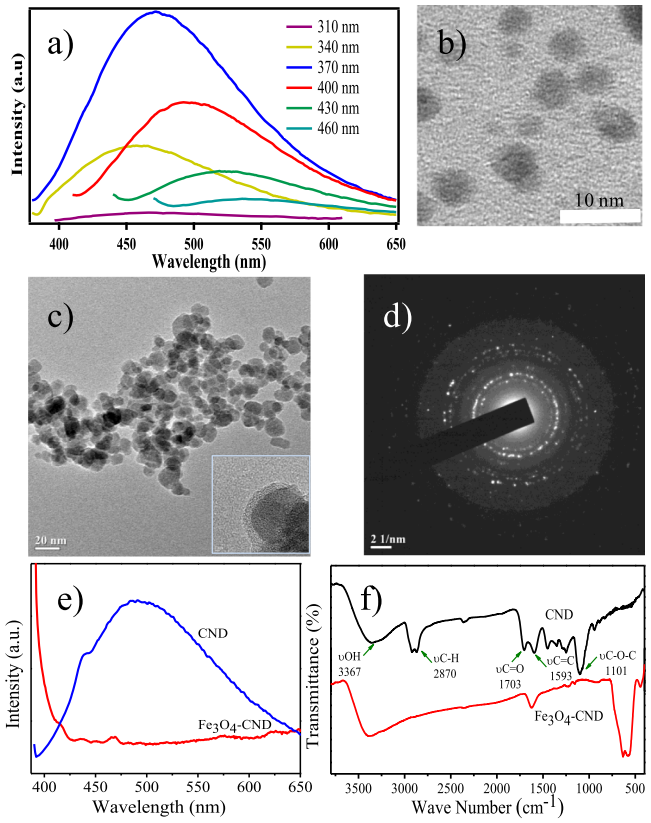

Figure 1. (a) Excitation-dependent emission spectrum of CNDs, (b,c) TEM images of CNDs and Fe_3O_4−CNDs; HRTEM image of Fe_3O_4−CNDs (inset c), (d) SAED pattern for Fe_3O_4−CNDs, and (e,f) emission and FTIR spectra of CNDs and Fe_3O_4−CNDs, respectively.

low-contrast continuous CND layer of thickness ca. 2.6 nm, as observed by high-resolution TEM (HRTEM), signifying the formation of a core−shell structure (inset Figure 1c). The Fe_3O_4−CND showed high crystallinity as demonstrated by the selected area electron diffraction (SAED) pattern (Figure 1d). The effective coating of CNDs on the Fe_3O_4 surface was further evidenced by the quenching of fluorescence owing to CNDs (Figure 1e). It is well-known that CNDs show high fluorescence selectivity for Fe^{3+} ions because of fast electron transfer between Fe^{3+} and CNDs surface-passivated with oxygen-rich groups.[48] The fluorescence of CNDs quenches because of the resulting nonradiative electron/hole recombination. Further evidence for the CND binding to the iron oxide surface was obtained from the Fourier transform infrared (FTIR) studies. The peak intensity of the oxygenated functional groups of CNDs such as −C═O and C−O−C (~1703 and 1101 cm^{-1}) was decreased significantly in the Fe_3O_4−CND composite, indicating the involvement of these groups in surface stabilization. In addition, a new peak at ~594 cm^{-1} corresponding to Fe−O stretching was also observed (Figure 1f). Scanning electron microscopy image and energy-dispersive spectroscopic analysis revealed the presence of C, O, and Fe in the composite material (Figure S1). Powder X-ray diffraction (PXRD), magnetic susceptibility measurement, and X-ray photoelectron spectroscopy (XPS) were performed to obtain the physicochemical properties of the nanocomposite. PXRD studies showed the characteristic Bragg's reflections corresponding to Fe_3O_4 along with a broad peak at $2\theta = 23°$, reflecting the presence of CNDs (Figure 2a).[49,50] Magnetic susceptibility measurement of Fe_3O_4−CND composite (Figure 2b) showed a reduced magnetization value (48.6 emu/g) compared to that of earlier reported bare Fe_3O_4 NPs (64 emu/g).[51] Moreover, remanence on the magnetization loop, zero coercivity, and the absence of a hysteresis loop suggested that the Fe_3O_4−CND composite showed a superparamagnetic behavior.

We further performed XPS measurements of the synthesized nanocomposite. The XPS survey spectrum of Fe_3O_4−CND composite shows major lines at binding energies (BEs) of about 284.6, 530.7, and 710.7−724.6 eV which can be attributed to C 1s, O 1s, and Fe 2p, respectively (Figure 3a).[52] XPS signals appearing at BEs 710.7 and 724.6 eV corresponding to Fe $2p_{3/2}$ and Fe $2p_{1/2}$ levels, respectively, are characteristic peaks for Fe_3O_4 nanoparticles (Figure 3b). The C 1s core-level spectrum of Fe_3O_4−CND composite could be fitted into four components having BEs at about 284.8, 286.2, 287.9, and 289.0 eV that can be attributed to the non-oxygenated carbon in C−C, epoxy carbon in C−O, carbonyl carbon in C═O, and carboxyl carbon in O−C═O, respectively (Figure 3c). The O 1s core-level spectrum of Fe_3O_4−CND composite was fitted into three components with BEs at about 530.7, 532.2, and 533.2 eV, which correspond to the anionic oxygen in Fe_3O_4, carbonyl oxygen in C═O, and alkoxy oxygen in C−O, respectively (Figure 3d).

Cyclooxidative Synthesis of Quinazolinone. An environmentally friendly methodology for the formation of quinazolinones using a recyclable and heterogeneous catalyst in aqueous medium is of utmost importance. The use of alcohols as starting materials represents a more benignant pathway compared to unstable aldehydes. The catalytic activity of Fe_3O_4−CND composite was initially evaluated by studying the coupling of benzyl alcohol (1a) with 2-aminobenzamide

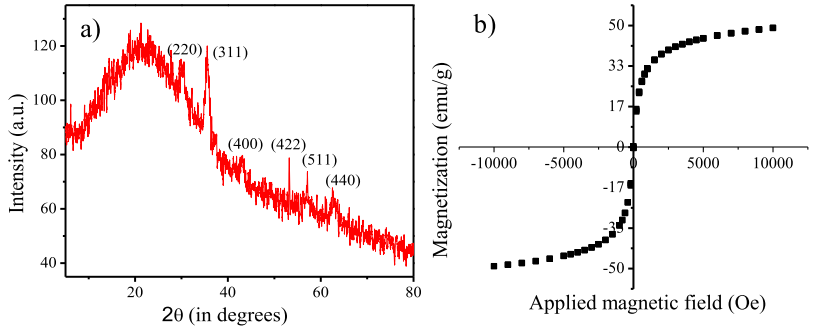

Figure 2. (a) PXRD pattern and (b) magnetization curve for CND-stabilized iron oxide nanoparticles.

DOI: 10.1021/acsomega.8b01794
ACS Omega 2018, 3, 13711−13719

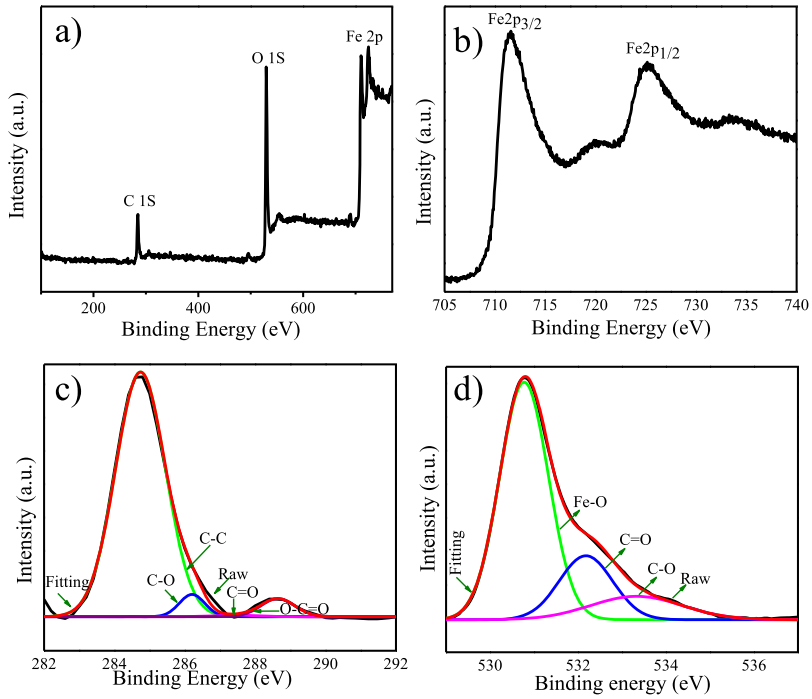

Figure 3. (a) Wide-scan XPS spectrum of Fe_3O_4−CND, (b) Fe 2p, (c) C 1s, and (d) O 1s core-level XPS spectrum of Fe_3O_4−CND composite.

(2a) as a model reaction in aqueous medium. The use of molecular oxygen as the terminal oxidant resulted in poor conversion with dihydroquinazolinone as the major product. On the other hand, the use of TBHP replacing O_2 as the oxidant resulted in high conversion with quinazolinone as the major product (Scheme 2).

Scheme 2. C−H Amidation Leading to Dihydroquinazolinone and Quinazolinone

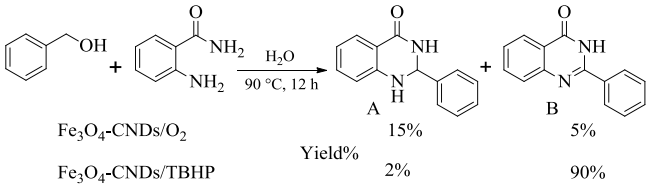

With these encouraging results in hand, we optimized the reaction conditions to obtain the suitable reaction parameters. In the presence of nanocatalysts, the reaction resulted in no product formation at room temperature in an aqueous medium (Table 1, entry 1). However, increasing the reaction temperature to 90 °C using molecular oxygen as the terminal oxidant resulted in the desired quinazolinone product with 5% yield. Further, the use of H_2O_2 as the oxidant resulted only in trace amount of quinazolinone formation. Changing the external oxidant to TBHP (2 equiv) instead of molecular oxygen or H_2O_2 resulted in a significant enhancement in the reaction rate and resulted in 94% of quinazolinone (Table 1, entry 4). In a controlled reaction, only TBHP in the absence of catalyst resulted in 25% of the product (Table 1, entry 5). Further, the model reaction using CNDs as a catalyst (without Fe_3O_4) in the presence of TBHP at 90 °C afforded 35% yield of the desired product (Table 1, entry 7). Reactions with variable catalyst loading showed that 10 wt % of Fe_3O_4−CND nanocatalyst to be optimal for the reaction (Tables 1 and S1).

Table 1. Oxidative Coupling of (1a) and (2a) under Various Conditions[a]

entry	catalyst (wt %)	solvent	oxidant (equiv)	T (°C)	yield[b] (%)
1	Fe_3O_4−CND (10)	H_2O		r.t	Nr
2	Fe_3O_4−CND (10)	H_2O		90	5
3	Fe_3O_4−CND (10)	H_2O	TBHP (1)	90	62
4	Fe_3O_4−CND (10)	H_2O	TBHP (2)	90	94
5		H_2O	TBHP (2)	90	25
6	Fe_3O_4−CND (10)	CH_3CN	H2O2 (2)	90	trace
7	CND (10)	H_2O	TBHP (2)	90	35
8	Fe_3O_4−CND (10)	$PhCH_3$	TBHP (2)	90	95
9	Fe_3O_4−CND (10)	C_2H_5OH	TBHP (2)	90	65
10	Fe_3O_4 (10)	H_2O	TBHP (2)	90	57
11	Fe_3O_4−citrate (10)	H_2O	TBHP (2)	90	60

[a]Reaction conditions: 1a (1.5 mmol), 2a (0.5 mmol), oxidant 1−2 equiv and solvent 2 mL, 16 h. [b]Yields of isolated product.

Among the solvents screened, although toluene gave comparable product yield with that of water, we chose water as the solvent for our further studies. Increase in the amount of TBHP to 4 equiv had detrimental effect on the reaction as lower yield of the product was obtained (Table S1, entry 5). The use of bare Fe_3O_4 NPs as the catalyst resulted only in 57% yield of the product (Table 1, entry 10). This can be attributed to the possible agglomeration of the NPs under thermal reaction conditions. Further, citrate-stabilized Fe_3O_4 NPs resulted in 60% yield of quinazolinone under similar reaction conditions (Table 1, entry 11). An inorganic base, similar to K_2CO_3, was found to be ineffective for the reaction and

DOI: 10.1021/acsomega.8b01794
ACS Omega 2018, 3, 13711−13719

Table 2. Synthesis of Quinazolinones Catalyzed by Fe_3O_4−CND composite[a]

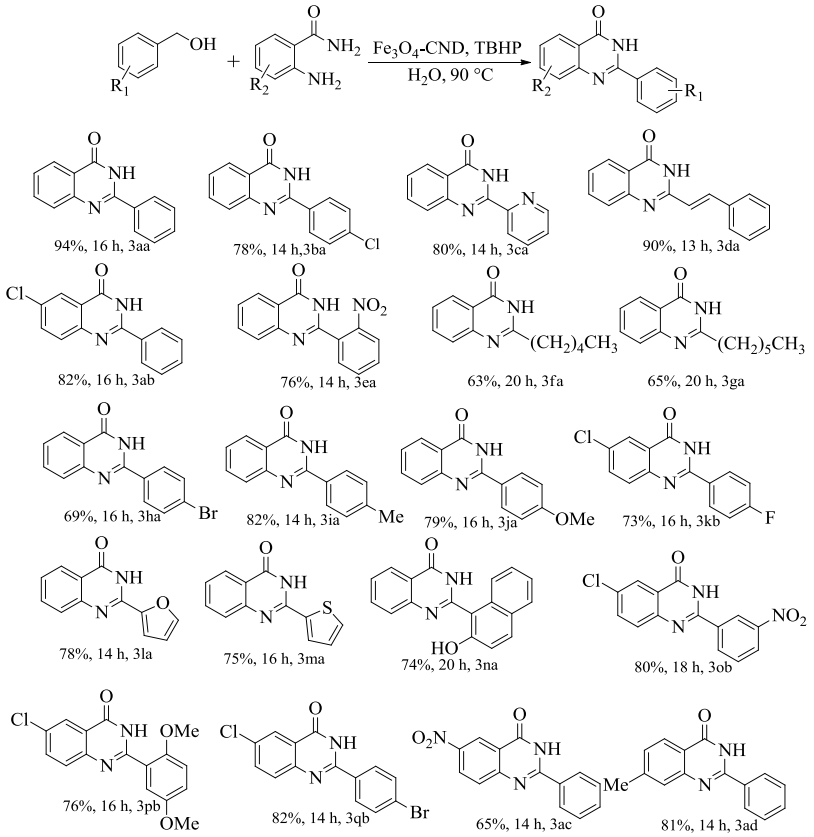

[a]Reaction conditions: alcohol (1.5 mmol), 2-aminobenzamide (0.5 mmol), 10 wt % Fe_3O_4−CND, 2.0 equiv TBHP, and 2 mL of water, magnetically stirred at 900 rpm, 13−20 h at 90 °C.

resulted only in trace formation of the product (Table S1, entry 6). Overall, the optimal reaction condition was obtained using 10 wt % of Fe_3O_4−CND catalyst in the presence of TBHP as the oxidant at 90 °C for 16 h in aqueous medium.

Having the optimized reaction conditions in hand, we evaluated the substrate scope for the reaction. Various primary alcohols were used as substrates to react with 2-aminobenzamide (2a), and the results are summarized in Table 2. A wide range of quinazolinones could be synthesized with good to excellent yields under the present reaction condition. Benzyl alcohol bearing electronically activating substituent such as −Me and −OMe could be coupled with 2-aminobenzamide to give excellent yield of their corresponding quinazolinone products (82 and 79%, 3ia, 3ja, Table 2), whereas those with electronically deactivating substituent $-NO_2$ resulted in comparatively lesser yield of the product (76%, 3ea, Table 2). Halo-substituted benzyl alcohols were also found to be stable under the reaction conditions and could be introduced in the quinazolinone skeleton with excellent yields (entry 3ba, 3ha, and 3kb, Table 2). In the case of cinnamyl alcohol, the olefinic C═C bond survived well under the reaction conditions and resulted in corresponding quinazolinone with 90% yield (entry 3da, Table 2). Several substituted 2-aminobenzamides were also found to be compatible under the present reaction conditions and several primary alcohols with electronically rich/poor/halo substituents could be converted to the desired products with excellent yields (3ab, 3kb, 3ob, 3pb, 3qb, 3ac, and 3ad, Table 2). Heteroatoms are known to poison the metal oxide surface by strongly coordinating to the active catalytic site. However, heterocyclic alcohols such as 2-pyridine carboxaldehyde, furfural, and 2-thiophenecarboxaldehyde could be efficiently transformed into the desired products with high yields using the present synthetic protocol (entry 3ca, 3la, and 3ma, Table 2). Fused ring alcohol could also be transformed to the desired quinazolinone skeleton with 74% yield (entry 3na, Table 2). Furthermore, inactive aliphatic alcohols could also be coupled to give the desired product with reasonably good yields (entry 3fa and 3ga, Table 2).

On the other hand, when benzylamine was allowed to react with 2-aminobenzamide under the optimized reaction condition, the corresponding quinazolinone product was obtained with ∼80% yield; however, several byproducts were obtained including benzaldehyde, imine, and 2,3-dihydroquinazolinone. Similarly, when 2-aminobenzylamine was allowed to react with benzyl alcohol under the same reaction condition, the corresponding quinazoline product was obtained with 55% yield.

Mechanistic Studies. A few control experiments were carried out to have an insight into the reaction mechanism (Scheme 3). Reaction of benzaldehyde and 2-aminobenzamide in the presence Fe_3O_4−CND and TBHP yielded quinazolinone as the exclusive product, whereas in their absence resulted in dihydroquinazolinone as the major product.[53,54] The results suggest that benzaldehyde and dihydroquinazolinone could be the intermediates in the model coupling reaction of benzyl alcohol and 2-aminobenzamide.

DOI: 10.1021/acsomega.8b01794
ACS Omega 2018, 3, 13711−13719

Scheme 3. Control Experiments with Benzaldehyde and 2-Aminobenzamide as Starting Materials

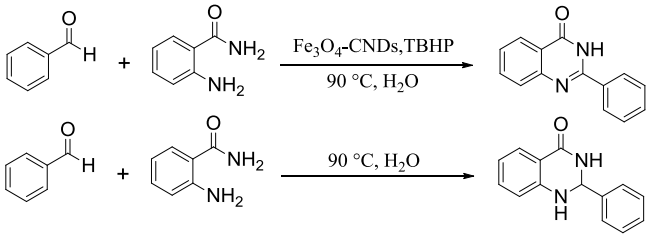

Further, the reaction was significantly inhibited when radical inhibitors such as (2,2,6,6-tetramethylpiperidin-1-yl)oxy and butylated hydroxytoluene (BHT) were added to the reaction (Schemes 4 and 5). This result indicates that the reaction should follow a free-radical pathway.[55−59]

Scheme 4. Presence of Radical Inhibitor Indicating a Free-Radical Process

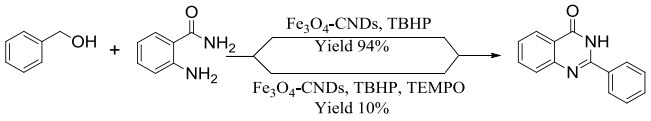

Scheme 5. All Reactions were Carried out Using 0.5 mmol Substrate, 1.0 mmol TBHP, 0.5 mmol BHT, 10 mg of Catalyst and 2 mL of Water at 90 °C, Rate in the Unit of 10^{-5} mol/s

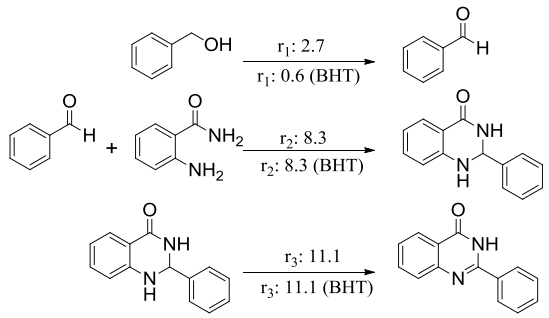

On the basis of these results, we propose a reaction sequence for the cyclooxidative tandem reaction of benzyl alcohol and 2-aminobenzamide (Scheme 5). In the first step, oxidation of benzyl alcohol resulted in the formation of benzaldehyde, which reacts with 2-aminobenzamide to generate dihydroquinazolinone (step 2). Finally, dihydroquinazolinone oxidizes to give the final product quinazolinone. Oxidation of benzyl alcohol to benzaldehyde (step 1), which is the rate-determining step, involves free radicals because the presence of free-radical scavengers such as BHT greatly reduced the reaction rate. Oxidation of dihydroquinazolinone (step 3) does not involve any radical process as the corresponding reaction rate was not affected by the presence of BHT.

It is well-reported that reactive oxygen species (ROS) derived from TBHP or other peroxides are short-lived in solution, and the stoichiometric amount of TBHP is usually required to maintain significant ROS concentration for a longer period.[60] However, these ROS can have extended stability on nanoparticle surface with enhanced lifetime that can facilitate the oxidation reactions.[61] In our case, the unprecedented catalytic activity of the Fe_3O_4−CND and TBHP system may be attributed to the rapid decomposition of TBHP to its radicals catalyzed by Fe_3O_4−CND and their enhanced stability on the nanoparticle surface. Further, the enhanced activity of Fe_3O_4−CND nanocomposite compared to bare or citrate-stabilized Fe_3O_4 NPs toward the formation of quinazolinones could be attributed to the cooperativity between CND and Fe_3O_4 NPs, as CNDs are known to have intrinsic peroxidase activities.

Reusability Studies. The superparamagnetic nature of Fe_3O_4−CND permits recovery of the catalyst from the reaction mixture easily with the help of a simple magnet without the loss of catalyst mass (Figure 4a). The reusability of the recovered catalyst was evaluated for the model reaction, and more than 90% of its original activity was retained even after four cycles (Figure 4b). Morphological studies of Fe_3O_4−CND recovered after the third cycle of reaction showed no significant changes in the particle morphology (Figure 4c). On the other hand, a significant decrease in the catalytic activity was observed for recovered bare Fe_3O_4 NPs (34%) or Fe_3O_4−citrate (43%) because of the loss of structural integrity even after the first cycle.

Further, we performed a leaching test to investigate the stability of the nanocomposite during the catalytic reaction (Figure 5). In the leaching test, the reaction was stopped after 4 h, and the catalyst was removed using a magnet. The reaction was further continued with the filtrate. However, after the stipulated time of 16 h, we did not observe any increment in product formation which clearly suggests that no active species were leached during the course of the catalytic reaction.

CONCLUSIONS

In summary, CND-stabilized magnetic iron oxide nanoparticle composite has been demonstrated as an effective catalytic system for a one-pot cascade quinazolinone synthesis in aqueous medium from alcohols and 2-aminobenzamides in a cyclooxidative pathway in the presence of TBHP. The rapid decomposition of TBHP into its radicals (ROS) and their

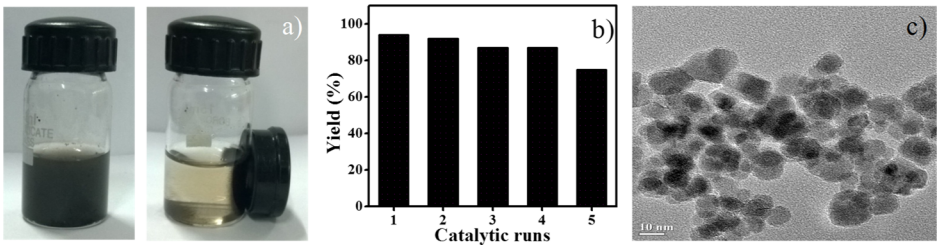

Figure 4. (a) Digital image showing dispersion of Fe_3O_4−CND nanoparticles in the presence and absence of external magnet, (b) reusability study of Fe_3O_4−CND for the model reaction, and (c) TEM image of Fe_3O_4−CND recovered after the third cycle of reaction.

DOI: 10.1021/acsomega.8b01794
ACS Omega 2018, 3, 13711−13719

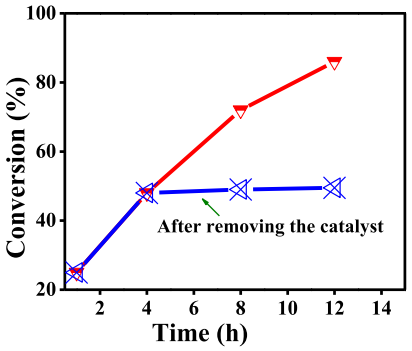

Figure 5. Leaching test indicating no leaching of active species from the catalysts during catalytic reaction.

surface stabilization on the nanoparticle account for the exceptional catalytic activity of the system. Further, the inherent magnetic nature of the catalytic system renders easy recovery of the catalyst from the reaction mixture that can be reused with efficient activity over several cycles. The results demonstrate excellent synergistic effect of carbon dots with metal oxide nanoparticles that can be harnessed for important heterogeneous organic transformations.

EXPERIMENTAL DETAILS

Generation Information. A Bruker D8 ADVANCE X-ray diffractometer with Cu Kα source (0.154 nm wavelength) was used to perform powder XRD analysis of the nanocatalysts. A JEOL JEM-2100 TEM microscope (200 kV) was used to obtain morphological analysis. UV−visible and FTIR measurements were performed by using Varian Cary 10 Bio Spectrophotometer and Bruker Tensor 27 instrument, respectively. FluoroMax-4p fluorometer from Horiba (model: FM-100) was used to record the emission spectra. XPS spectra were obtained from an ESCA instrument, VSW (UK). EverCool 7 T SQUID magnetometer was used to perform magnetic susceptibility measurements. All NMR analyses (^{1}H and ^{13}C) were done using Bruker ADVANCE (III) 400 or 100 MHz spectrometer, respectively. ^{1}H NMR assignment data are reported using the format chemical shift (δ ppm), multiplicity [singlet (s), doublet (d), triplet (t), and multiplet (m)], coupling constant (J Hz), and integration value. For ^{13}C NMR, only a chemical shift value is reported. ESI-TOF-MS was used to record high-resolution mass spectra.

Materials and Methods. PEG-200, used as a carbon source to synthesize CNDs, was purchased from Alfa Aesar. Iron sulfate, iron chloride, and sodium hydroxide were purchased from Merck, India. TBHP, hydrogen peroxide, and all other chemicals were purchased from Sigma-Aldrich and Merck India and used without further purification. We used Millipore water (ultrapure level) throughout the experiments.

Synthesis of Carbon Nanodots. In a typical method, 15 mL of PEG-200 in a sealed glass tube was subjected to microwave irradiation (focused microwave CEM discover reactor) at 150 W and 150 °C for 30 min. The colorless liquid turned into brown upon microwave treatment. The brown mixture was then diluted with 50 mL of water and dialyzed using a dialysis membrane (molecular cutoff of 10 kDa) for 48 h to remove unreacted materials. The CND containing solution was further centrifuged at 22 000 rpm and washed with water for several times. Finally, the carbon dots were redispersed in water to make a concentration of 0.5 mg mL^{-1} and used for further experiments.

Synthesis of Fe_3O_4−CND Nanocomposite. The synthesized CND solution (50 mL) was used as a reaction medium for the synthesis of iron oxide nanoparticles. Iron sulfate (2.0 mmol; 0.556 g) and iron chloride (4.0 mmol; 0.648 g) were added to a three-neck round-bottom flask containing CND solution. The flask containing the mixture was put on a magnetic stirrer and heated to 60 °C keeping the solution stirred. Any air (oxygen) present inside the flask was removed using a vacuum pump, and the flask was filled with inert nitrogen gas. To ensure complete removal of oxygen, we purged nitrogen gas three times into the flask and removed them using a vacuum pump. After 10 min, 20 mL of 2.5 M NaOH solution was added to the mixture using a syringe. This changed the solution color from brown to black, indicating the formation of iron oxide nanoparticles. After 12 h, the reaction was stopped and cooled. Iron oxide nanoparticles stabilized with CNDs settled on the bottom of the flask. The supernatant liquid was removed, and the catalyst was purified by washing with Milli-Q water and ethanol.

Cyclooxidative Synthesis of Quinazolinones. In a Teflon-sealed glass tube, 1.5 mmol alcohol, 0.5 mmol 2-aminobenzamide, 193 μL of TBHP, 25 mg of Fe_3O_4−CND, and 2 mL of H_2O were taken, and the mixture was heated at 90 °C in an oil bath under magnetic stirring for 13−20 h. The progress of the reaction was monitored by thin-layer chromatography. After completion of the reaction, the reaction was cooled to room temperature, and the catalyst was removed by using a magnet. The resulting mixture was extracted with ethyl acetate (3 × 20 mL) and successively washed with water (1 × 15 mL). The organic solution was dried over anhydrous sodium sulfate, and the solvent was evaporated using a rotary evaporator to get the crude reaction mixture. Further, the pure product was obtained by purifying the mixture on silica gel column chromatography (100−200 mesh) using hexane and ethyl acetate as the eluents.

ASSOCIATED CONTENT

Supporting Information

The Supporting Information is available free of charge on the ACS Publications website at DOI: 10.1021/acsomega.8b01794.

Additional figures, optimization data, characterization data, and NMR spectra of organic compounds (PDF)

AUTHOR INFORMATION

Corresponding Author

*E-mail: tridib@iiti.ac.in (T.K.S.).

ORCID

Tridib K. Sarma: 0000-0002-5168-6327

Notes

The authors declare no competing financial interest.

ACKNOWLEDGMENTS

We thank IIT Indore and SIC, IIT Indore, for providing funding and instrumentation facilities. B.M. thanks UGC, New Delhi, for fellowship. Instrumentation support from SAIF, NEHU, Shillong, UGC-DAE Consortium for Scientific Research, Indore, and IIT Kanpur are highly acknowledged.

DOI: 10.1021/acsomega.8b01794
ACS Omega 2018, 3, 13711−13719

REFERENCES

(1) Gawande, M. B.; Branco, P. S.; Varma, R. S. Nano-magnetite (Fe_3O_4) as a support for recyclable catalysts in the development of sustainable methodologies. *Chem. Soc. Rev.* **2013**, *42*, 3371−3393.

(2) Baig, R. B. N.; Varma, R. S. Magnetically retrievable catalysts for organic synthesis. *Chem. Commun.* **2013**, *49*, 752−770.

(3) Baig, R. B. N.; Varma, R. S. Organic synthesis via magnetic attraction: Benign and sustainable protocols using magnetic nano-ferrites. *Green Chem.* **2013**, *15*, 398−417.

(4) Le Bras, J.; Muzart, J. Intermolecular Dehydrogenative Heck Reactions. *Chem. Rev.* **2011**, *111*, 1170−1214.

(5) Wencel-Delord, J.; Dröge, T.; Liu, F.; Glorius, F. Towards mild metal-catalyzed C-H bond activation. *Chem. Soc. Rev.* **2011**, *40*, 4740−4761.

(6) Song, G.; Wang, F.; Li, X. C-C, C-O and C-N bond formation via rhodium(iii)-catalyzed oxidative C-H activation. *Chem. Soc. Rev.* **2012**, *41*, 3651−3678.

(7) Arockiam, P. B.; Bruneau, C.; Dixneuf, P. H. Ruthenium(II)-Catalyzed C-H Bond Activation and Functionalization. *Chem. Rev.* **2012**, *112*, 5879−5918.

(8) Luo, J.; Wei, W.-T. Recent Advances in the Construction of C-N Bonds Through Coupling Reactions between Carbon Radicals and Nitrogen Radicals. *Adv. Synth. Catal.* **2018**, *360*, 2076−2086.

(9) Horton, D. A.; Bourne, G. T.; Smythe, M. L. The combinatorial synthesis of bicyclic privileged structures or privileged substructures. *Chem. Rev.* **2003**, *103*, 893−930.

(10) Huang, C.; Fu, Y.; Fu, H.; Jiang, Y.; Zhao, Y. Highly efficient copper-catalyzed cascade synthesis of quinazoline and quinazolinone derivatives. *Chem. Commun.* **2008**, 6333−6335.

(11) Xu, L.; Jiang, Y.; Ma, D. Synthesis of 3-Substituted and 2,3-Disubstituted Quinazolinones via Cu-Catalyzed Aryl Amidation. *Org. Lett.* **2012**, *14*, 1150−1153.

(12) Voelter, W.; Abdel-Jail, R. J.; Aldoqum, H. M.; Ayoub, M. T. Synthesis and antitumor activity of 2-aryl-7-fluoro-6-(4-methyl-1-piperazinyl)-4(3H)-quinazolinones. *Heterocycles* **2005**, *65*, 2061−2070.

(13) Mitobe, Y.; Ito, S.; Mizutani, T.; Nagase, T.; Sato, N.; Tokita, S. Development of a selective and potent radioactive ligand for histamine H_3 receptors: A compound potentially useful for receptor occupancy Studies. *Bioorg. Med. Chem. Lett.* **2009**, *19*, 4075−4078.

(14) Ge, W.; Zhu, X.; Wei, Y. Iodine-catalyzed oxidative system for cyclization of primary alcohols with o-aminobenzamides to quinazolinones using DMSO as the oxidant in dimethyl carbonate. *RSC Adv.* **2013**, *3*, 10817−10822.

(15) Sharif, M.; Opalach, J.; Langer, P.; Beller, M.; Wu, X.-F. Oxidative synthesis of quinazolinones and benzothiadiazine 1,1-dioxides from 2-aminobenzamide and 2-aminobenzenesulfonamide with benzyl alcohols and aldehydes. *RSC Adv.* **2014**, *4*, 8−17.

(16) Watson, A. J. A.; Maxwell, A. C.; Williams, J. M. J. Ruthenium-catalysed oxidative synthesis of heterocycles from alcohols. *Org. Biomol. Chem.* **2012**, *10*, 240−243.

(17) Hikawa, H.; Ino, Y.; Suzuki, H.; Yokoyama, Y. Pd-Catalyzed Benzylic C-H Amidation with Benzyl Alcohols in Water: A Strategy To Construct Quinazolinones. *J. Org. Chem.* **2012**, *77*, 7046−7051.

(18) Hu, Y.; Chen, L.; Li, B. Iron nitrate/TEMPO-catalyzed aerobic oxidative synthesis of quinazolinones from alcohols and 2-amino-benzamides with air as the oxidant. *RSC Adv.* **2016**, *6*, 65196−65204.

(19) Zhao, D.; Zhou, Y.-R.; Shen, Q.; Li, J.-X. Iron-catalyzed oxidative synthesis of N-heterocycles from primary alcohols. *RSC Adv.* **2014**, *4*, 6486−6489.

(20) Siddiki, S. M. A. H.; Kon, K.; Touchy, A. S.; Shimizu, K.-i. Direct synthesis of quinazolinones by acceptorless dehydrogenative coupling of o-aminobenzamide and alcohols by heterogeneous Pt catalysts. *Catal. Sci. Technol.* **2014**, *4*, 1716−1719.

(21) Zhou, J.; Fang, J. One-Pot Synthesis of Quinazolinones via Iridium-Catalyzed Hydrogen Transfers. *J. Org. Chem.* **2011**, *76*, 7730−7736.

(22) Gujjarappa, R.; Maity, S. K.; Hazra, C. K.; Vodnala, N.; Dhiman, S.; Kumar, A.; Beifuss, U.; Malakar, C. C. Divergent Synthesis of Quinazolines Using Organocatalytic Domino Strategies under Aerobic Conditions. *Eur. J. Org. Chem.* **2018**, *2018*, 4628−4638.

(23) Ma, J.; Wan, Y.; Hong, C.; Li, M.; Hu, X.; Mo, W.; Hu, B.; Sun, N.; Jin, L.; Shen, Z. ABNO-Catalyzed Aerobic Oxidative Synthesis of 2-Substituted 4H -3,1-Benzoxazines and Quinazolines. *Eur. J. Org. Chem.* **2017**, *2017*, 3335−3342.

(24) Xie, L.-Y.; Duan, Y.; Lu, L.-H.; Li, Y.-J.; Peng, S.; Wu, C.; Liu, K.-J.; Wang, Z.; He, W.-M. Fast, Base-Free and Aqueous Synthesis of Quinolin-2(1H)-ones under Ambient Conditions. *ACS Sustainable Chem. Eng.* **2017**, *5*, 10407−10412.

(25) Wei, W.-T.; Zhu, W.-M.; Bao, W.-H.; Chen, W.-T.; Huang, Y.-L.; Gao, L.-H.; Xu, X.-D.; Wang, Y.-N.; Chen, G.-P. Metal-Free $C(sp^3)$−H Amination of 2-Oxindoles in Water: Facile Synthesis of 3-Substituted 3-Aminooxindoles. *ACS Sustainable Chem. Eng.* **2018**, *6*, 5615−5619.

(26) Wei, W.-T.; Zhu, W.-M.; Shao, Q.; Bao, W.-H.; Chen, W.-T.; Chen, G.-P.; Luo, Y.-J.; Liang, H. Transition-Metal-Free $C(sp^3)$−H Hydroxylation of 2-Oxindoles with Peroxides via Radical Cross-Coupling Reaction in Water. *ACS Sustainable Chem. Eng.* **2018**, *6*, 8029−8033.

(27) Xie, L.-Y.; Li, Y.-J.; Qu, J.; Duan, Y.; Hu, J.; Liu, K.-J.; Cao, Z.; He, W.-M. A base-free, ultrasound accelerated one-pot synthesis of 2-sulfonylquinolines in water. *Green Chem.* **2017**, *19*, 5642−5646.

(28) Wei, W.-T.; Zhu, W.-M.; Ying, W.-W.; Wu, Y.; Huang, Y.-L.; Liang, H. Metal-free synthesis of isatin oximes via radical coupling reactions of oxindoles with t-BuONO in water. *Org. Biomol. Chem.* **2017**, *15*, 5254−5257.

(29) Butler, R. N.; Coyne, A. G. Water: Nature's Reaction Enforcer-Comparative Effects for Organic Synthesis "In-Water" and "On-Water". *Chem. Rev.* **2010**, *110*, 6302−6337.

(30) Hudson, R.; Feng, Y.; Varma, R. S.; Moores, A. Bare magnetic nanoparticles: sustainable synthesis and applications in catalytic organic transformations. *Green Chem.* **2014**, *16*, 4493−4505.

(31) Gawande, M. B.; Luque, R.; Zboril, R. The rise of magnetically recyclable nanocatalysts. *ChemCatChem* **2014**, *6*, 3312−3313.

(32) Sharma, R. K.; Dutta, S.; Sharma, S.; Zboril, R.; Varma, R. S.; Gawande, M. B. Fe_3O_4 (iron oxide)-supported nanocatalysts: synthesis, characterization and applications in coupling reactions. *Green Chem.* **2016**, *18*, 3184−3209.

(33) Wang, D.; Astruc, D. Fast-growing field of magnetically recyclable nanocatalysts. *Chem. Rev.* **2014**, *114*, 6949−6985.

(34) Wang, R.; Lu, K.-Q.; Tang, Z.-R.; Xu, Y.-J. Recent progress in carbon quantum dots: synthesis, properties and applications in photocatalysis. *J. Mater. Chem. A* **2017**, *5*, 3717−3734.

(35) Sun, H.; Wu, L.; Wei, W.; Qu, X. Recent advances in graphene quantum dots for sensing. *Mater. Today* **2013**, *16*, 433−442.

(36) Bak, S.; Kim, D.; Lee, H. Graphene quantum dots and their possible energy applications: A review. *Curr. Appl. Phys.* **2016**, *16*, 1192−1201.

(37) Shen, J.; Zhu, Y.; Yang, X.; Li, C. Graphene quantum dots: emergent nanolights for bioimaging, sensors, catalysis and photovoltaic devices. *Chem. Commun.* **2012**, *48*, 3686−3699.

(38) Wang, Y.; Hu, A. Carbon quantum dots: synthesis, properties and applications. *J. Mater. Chem. C* **2014**, *2*, 6921−6939.

(39) Shi, W.; Wang, Q.; Long, Y.; Cheng, Z.; Chen, S.; Zheng, H.; Huang, Y. Carbon nanodots as peroxidase mimetics and their applications to glucose detection. *Chem. Commun.* **2011**, *47*, 6695−6697.

(40) Sun, H.; Zhao, A.; Gao, N.; Li, K.; Ren, J.; Qu, X. Deciphering a Nanocarbon-Based Artificial Peroxidase: Chemical Identification of the Catalytically Active and Substrate-Binding Sites on Graphene Quantum Dots. *Angew. Chem., Int. Ed.* **2015**, *54*, 7176−7180.

(41) Dey, D.; Bhattacharya, T.; Majumdar, B.; Mandani, S.; Sharma, B.; Sarma, T. K. Carbon dot reduced palladium nanoparticles as active catalysts for carbon-carbon bond formation. *Dalton Trans.* **2013**, *42*, 13821−13825.

(42) Mandani, S.; Sharma, B.; Dey, D.; Sarma, T. K. Carbon nanodots as ligand exchange probes in Au@C-dot nanobeacons for

DOI: 10.1021/acsomega.8b01794
ACS Omega 2018, 3, 13711−13719

fluorescent turn-on detection of biothiols. *Nanoscale* **2015**, *7*, 1802−1808.
(43) Su, D. S.; Perathoner, S.; Centi, G. Nanocarbons for the development of advanced catalysts. *Chem. Rev.* **2013**, *113*, 5782−5816.
(44) Majumdar, B.; Mandani, S.; Bhattacharya, T.; Sarma, D.; Sarma, T. K. Probing carbocatalytic activity of carbon nanodots for the synthesis of biologically active dihydro/spiro/glyco quinazolinones and aza-Michael adducts. *J. Org. Chem.* **2017**, *82*, 2097−2106.
(45) Zhang, Z.; Wang, M.; Zhang, C.; Zhang, Z.; Lu, J.; Wang, F. The cascade synthesis of quinazolinones and quinazolines using an α-MnO_2 catalyst and *tert*-butyl hydroperoxide (TBHP) as an oxidant. *Chem. Commun.* **2015**, *51*, 9205−9207.
(46) Gan, Z.; Xu, H.; Hao, Y. Mechanism for excitation-dependent photoluminescence from graphene quantum dots and other graphene oxide derivates: consensus, debates and challenges. *Nanoscale* **2016**, *8*, 7794−7807.
(47) Jaiswal, A.; Ghosh, S. S.; Chattopadhyay, A. One step synthesis of C-dots by microwave mediated caramelization of poly(ethylene glycol). *Chem. Commun.* **2012**, *48*, 407−409.
(48) Gong, X.; Lu, W.; Paau, M. C.; Hu, Q.; Wu, X.; Shuang, S.; Dong, C.; Choi, M. M. F. Facile synthesis of nitrogen-doped carbon dots for Fe(3+) sensing and cellular imaging. *Anal. Chim. Acta* **2015**, *861*, 74−84.
(49) Baig, R. B. N.; Nadagouda, M. N.; Varma, R. S. Carbon-coated magnetic palladium: applications in partial oxidation of alcohols and coupling reactions. *Green Chem.* **2014**, *16*, 4333−4338.
(50) Wang, H.; Wei, Z.; Matsui, H.; Zhou, S. Fe_3O_4/carbon quantum dots hybrid nanoflowers for highly active and recyclable visible-light driven photocatalyst. *J. Mater. Chem. A* **2014**, *2*, 15740−15745.
(51) Gholinejad, M.; Seyedhamzeh, M.; Razeghi, M.; Najera, C.; Kompany-Zareh, M. Iron oxide nanoparticles modified with carbon quantum nanodots for the stabilization of palladium nanoparticles: an efficient catalyst for the Suzuki reaction in aqueous media under mild conditions. *ChemCatChem* **2016**, *8*, 441−447.
(52) Hallam, P. M.; Gómez-Mingot, M.; Kampouris, D. K.; Banks, C. E. Facile synthetic fabrication of iron oxide particles and novel hydrogen superoxide supercapacitors. *RSC Adv.* **2012**, *2*, 6672−6679.
(53) Huang, D.; Li, X.; Xu, F.; Li, L.; Lin, X. Highly enantioselective synthesis of dihydroquinazolinones catalyzed by SPINOL-phosphoric acids. *ACS Catal.* **2013**, *3*, 2244−2247.
(54) Honjo, T.; Phipps, R. J.; Rauniyar, V.; Toste, F. D. A doubly axially chiral phosphoric acid catalyst for the asymmetric tandem oxyfluorination of enamides. *Angew. Chem., Int. Ed.* **2012**, *51*, 9684−9688.
(55) Wu, X.-F.; Bheeter, C. B.; Neumann, H.; Dixneuf, P. H.; Beller, M. Lewis acid-catalyzed oxidation of benzylamines to benzamides. *Chem. Commun.* **2012**, *48*, 12237−12239.
(56) Wang, L.; Zhu, H.; Guo, S.; Cheng, J.; Yu, J.-T. TBHP-promoted sequential radical silylation and aromatisation of aryl isonitriles with silanes. *Chem. Commun.* **2014**, *50*, 10864−10867.
(57) Tu, H.-Y.; Liu, Y.-R.; Chu, J.-J.; Hu, B.-L.; Zhang, X.-G. $FeCl_3$-promoted carboxamidation and cyclization of aryl isonitriles with formamides toward phenanthridine-6-carboxamides. *J. Org. Chem.* **2014**, *79*, 9907−9912.
(58) Ratnikov, M. O.; Doyle, M. P. Mechanistic investigation of oxidative Mannich reaction with tert-butyl hydroperoxide. The role of transition metal salt. *J. Am. Chem. Soc.* **2013**, *135*, 1549−1557.
(59) Luo, J.-Y.; Hua, H.-L.; Chen, Z.-S.; Zhou, Z.-Z.; Yang, Y.-F.; Zhou, P.-X.; He, Y.-T.; Liu, X.-Y.; Liang, Y.-M. Metal-free cascade radical cyclization of 1,6-enynes with aldehydes. *Chem. Commun.* **2014**, *50*, 1564−1566.
(60) Tan, J.; Zheng, T.; Yu, Y.; Xu, K. TBHP-promoted direct oxidation reaction of benzylic Csp^3−H bonds to ketones. *RSC Adv.* **2017**, *7*, 15176−15180.
(61) Saiman, M. I. b.; Brett, G. L.; Tiruvalam, R.; Forde, M. M.; Sharples, K.; Thetford, A.; Jenkins, R. L.; Dimitratos, N.; Lopez-Sanchez, J. A.; Murphy, D. M.; Bethell, D.; Willock, D. J.; Taylor, S. H.; Knight, D. W.; Kiely, C. J.; Hutchings, G. J. Involvement of surface-bound radicals in the oxidation of toluene using supported Au-Pd nanoparticles. *Angew. Chem., Int. Ed.* **2012**, *51*, 5981−5985.

DOI: 10.1021/acsomega.8b01794
ACS Omega 2018, 3, 13711−13719